The radio emission from active galactic nuclei

Radcliffe, J.F.; Barthel, P.D.; Garrett, M.A.; Beswick, R.J.; Thomson, A.P.; Muxlow, T.W.B.

Astronomy & Astrophysics manuscript no. Radio_silent_AGN_revision1
September 17, 2021

Letter to the Editor

The radio emission from Active Galactic Nuclei

J. F. Radcliffe[1,2,3], P. D. Barthel[1], M. A. Garrett[3,4], R. J. Beswick[3], A. P. Thomson[3], and T. W. B. Muxlow[3]

[1] Kapteyn Astronomical Institute, University of Groningen, 9747 AD Groningen, The Netherlands
e-mail: pdb@astro.rug.nl
[2] Department of Physics, University of Pretoria, Lynnwood Road, Hatfield, Pretoria, 0083, South Africa
[3] Jodrell Bank Centre for Astrophysics, School of Physics & Astronomy, The University of Manchester, Alan Turing Building, Oxford Road, Manchester M13 9PL, UK
[4] Leiden Observatory, Leiden University, PO Box 9513, 2300 RA Leiden, The Netherlands

Received xxx; accepted xxx

ABSTRACT

Context. For nearly seven decades astronomers have been studying active galaxies, that is to say galaxies with actively accreting central supermassive black holes, AGN. A small fraction of these are characterized by luminous, powerful radio emission: this class is known as radio-loud. A substantial fraction, the so-called radio-quiet AGN population, displays intermediate or weak radio emission. However, an appreciable fraction of strong X-rays emitting AGN are characterized by the absence of radio emission, down to an upper limit of about 10^{-7} times the luminosity of the most powerful radio-loud AGN.
Aims. We wish to address the nature of these – seemingly radio-silent – X-ray-luminous AGN and their host galaxies: is there any radio emission, and if so, where does it originate?
Methods. Focusing on the GOODS-N field, we examine the nature of these objects employing stacking techniques on ultra-deep radio data obtained with the JVLA. We combine these radio data with *Spitzer* far-infrared data.
Results. We establish the absence, or totally insignificant contribution of jet-driven radio-emission in roughly half of the otherwise normal population of X-ray luminous AGN, which appear to reside in normal star-forming galaxies.
Conclusions. AGN- or jet-driven radio emission is simply a mechanism that may be at work or may be dormant in galaxies with actively accreting black holes. The latter can be classified as radio-silent AGN.

Key words. galaxies: active – galaxies: jets – radio continuum: galaxies – X-rays: galaxies

1. Introduction: AGN in the radio sky

Emitting hundreds to thousands of radio flux units – Janskys – active galaxies and active galactic nuclei, AGN, were originally discovered through their luminous radio emission. It was however realized early that radio-loudness in active galaxies is the exception rather than the rule. For instance, many optically identified quasi-stellar objects, QSOs, were reported (Sandage 1965) to show no sign of radio emission. Following decades of research into the nature of this radio-quiet QSO population, a recent ultra-deep study by Kellermann et al. (2016) suggested that the 6 GHz radio luminosity function of optically selected low-redshift SDSS QSOs is primarily composed of two components. The first one is the AGN, jet-driven component that smoothly covers the (6 GHz) radio luminosity range from about 10^{27} down to 10^{23} W Hz^{-1}. The second one – which is prominently present in the sample – is the QSO host galaxy, starburst-driven radio emission, covering the 10^{21}–10^{23} W Hz^{-1} range. The latter emission is indicative of the formation of a few to several tens of (solar mass) stars per year. The host galaxy is responsible for the dominant radio emission component in approximately 80% of the sample – these objects make up the so-called "radio-quiet" QSO population. Lacking sufficient angular resolution, the standard connected interferometers like the VLA and the now operational SKA precursors are unable to quantify any low-level AGN-driven radio emission in these radio-quiet objects, that is to say jet-driven radio emission in the range 10^{21}–10^{22} W Hz^{-1}. For nearby low-luminosity AGN, that decomposition can successfully be made, by exploiting the radio–far-infrared correlation (e.g. Wilson 1988; Barthel 2006), but the (multi-faceted) physical origin of the radio emission in the radio-quiet AGN population is still being debated (Panessa et al. 2019). We here examine these extra-galactic radio populations in more detail.

The extra-galactic radio sky is currently studied down to microJy depths (e.g. Smolčić et al. 2017; Owen 2018; Mauch et al. 2020). The sky surface density of the ultra-luminous 3C or 3CR objects is about one per 10 × 10 degrees. These radio sources, having projected dimensions up to hundreds of kiloparsecs, reach radio luminosities up to 10^{28} W Hz^{-1} (at 1.4 GHz) at redshifts, z, up to 2.8. All of these are identified with powerful AGN – radio galaxies and quasars. Another well-known radio survey, the NRAO VLA Sky Survey, NVSS (Condon et al. 1998), goes about a factor of thousand deeper, to the mJy regime, and shows a source surface density of about one per $10' \times 10'$, with sources having radio luminosities down to about 10^{23} W Hz^{-1}. It is thought that the large majority of these radio sources are AGN driven. That situation changes when we go down another factor of hundred in depth. At arcsecond angular resolutions, the radio source surface density at the 10 μJy level is 2–4 per square arcmin. Slightly resolved starburst-driven radio sources, displaying alignment with their host galaxies and producing 10^{21}–10^{23} W Hz^{-1}, outnumber the AGN-driven objects at that level (e.g. Muxlow et al. 2005; Ibar et al. 2008; Padovani et al. 2009; Bonzini et al. 2013; Barger et al. 2015, 2017; Owen 2018; Ceraj et al. 2018; Mauch et al. 2020). This starburst dominance is also clearly seen as a sub-mJy upturn in the radio source counts (Smolčić et al. 2017), and in the ultra-deep radio survey of the general QSO population, discussed previously. Hence, identifying AGN in the sub-mJy radio population is not straightforward: they may occur at a low level in hybrid systems, or be absent.

Earlier, our team addressed these issues using the unique capacities of Very Long Baseline Interferometry (VLBI). Radcliffe et al. (2018) carried out ultra-deep wide-field VLBI in the GOODS-N (HDF-N) field, and reported the identification of 31 AGN in the redshift range 0.11–3.44 among hundreds of radio sources in that well-studied field. The Radcliffe et al. (in press.) follow-up study describes the nature of the host galaxies of the AGN and hybrid AGN-starburst systems: (1) AGN-dominated hybrid systems with efficient accretion, (2) intermediate redshift early-type hosts with inefficient AGN accretion, and (3) very dusty hybrid systems at high redshift, such as the well-known sub-mm source GN16.

Another important result of the Radcliffe et al. (in press) study is that about one third of the VLBI AGN remain undetected in the deep 2 Ms 0.5–7 keV *Chandra* X-ray observations (Xue et al. 2016). That fraction is in rough agreement with the fractional occurrence, or better absence, of X-ray emission in infrared-selected QSOs, as reported by Del Moro et al. (2016) and Mateos et al. (2017). Confirming the Padovani (2016) results, these X-ray deficient AGN occur in both distant passive, inefficiently accreting systems, and in very dusty host galaxies, which renders them weak or Compton-thick. The recent multiwavelength study by Lambrides et al. (2020) underlined the incompleteness of AGN X-ray studies.

However, while incomplete for certain AGN, X-ray surveys still yield the highest AGN[1] surface density, of about 7 per square arcmin (Luo et al. 2017). As reviewed by Brandt & Alexander (2015), X-ray surveys have been of utmost importance in AGN research, but the enigmatic aspect of the large X-ray surface density has not yet been solved: what is the nature of the luminous X-ray AGN without detectable radio emission? The issue is nicely illustrated by the detection statistics. Barger et al. (2017) find that the faint radio and deep *Chandra* X-ray populations are two disjunct populations, with only a certain level of overlap. Of the 445 1.4 GHz radio sources in the central 124 square arcmin of GOODS-N – AGN, starbursts, and mixed systems – 31% have X-ray counterparts (within 1.″5), and 69% have no X-ray counterparts. Of the GOODS-N X-ray sources down to $f_{0.5-2\mathrm{keV}} \approx 1.5 \times 10^{-17}$ erg cm^{-2} s^{-1} only 51% are associated with a (> 11.5 μJy) radio source. We here focus on the other half of the X-ray AGN – those which remain undetected in the radio.

2. Methods and results: radio-silent AGN?

To investigate the nature of the ultra-weak (or absent) radio emission of these X-ray bright sources, we carried out stacking techniques in our database for GOODS-N. We take advantage of the Owen (2018) ultra-deep (1.8 μJy beam^{-1}), 1–2 GHz JVLA observations, obtained as part of the *e*-MERGE survey, that have a resolution of approximately 1.″6 (Muxlow et al. 2020). There are 334 non-stellar sources in the 2 Ms *Chandra* GOODS-N catalogue with positional accuracy better than 0.″5 (Xue et al. 2016) which are also located within the *Spitzer*-MIPS 24 μm field of view. Of these, 168 sources (50.3%) have no VLA radio counterparts above a mean 5-sigma detection threshold of 10 μJy beam^{-1}, within a 1.″5 search radius. This detection fraction is entirely consistent with the results of Barger et al. (2017). To isolate a radio-silent population, we further filter these 168 non-detections using a Median Absolute Deviation (MAD) outlier filter (Iglewicz & Hoaglin 1993). For each pixel, x_i, in each 80×80 pixel radio image we compute the modified Z-score, M_i, using,

$$M_i = 0.6745 \frac{(x_i - \tilde{x})}{\mathrm{MAD}}, \quad (1)$$

where MAD = median($|x_i - \tilde{x}|$), and $\tilde{x}$ is the median of all the pixels in the image. Pixels are defined as outliers if $|M_i| > 3$ and a source image is rejected if there is an outlier pixel within 1.5 times the size of the VLA restoring beam ($\sim 2''$) from the X-ray position. This technique removes 78 sources with probable VLA counterparts with S/N of 3-5, that is to say peak brightness values of 6–10 μJy beam^{-1}. Finally, we exclude two sources that are behind extended radio emission from an FR-I radio galaxy. This yields a final sample of 88 X-ray sources (with known redshifts), or 26.3% of the original sample, that have a low probability of a radio counterpart. The redshift range of this sample is 0.079–5.186, with a mean value 1.54.

For each of these 88 X-ray sources, an 80×80 pixel ($28'' \times 28''$) cut-out centred on the X-ray position was excised. These images were aligned and a median and weighted mean stack (Figure 1a,b) was performed on a pixel-by-pixel basis. For the weighted mean stack, we added another MAD filter to identify and remove nearby sources. The weights used per image were proportional to the inverse square of the local rms noise. To ensure that the stacking routine was robust we performed a null test. For the same number of stacks, we added an additional random term (between $-15''$ and $+15''$) to the X-ray positions and, as Figure 1c shows, the stacking signal ceases to exist.

The median and weighted mean stacks in Figure 1 clearly show significant radio emission, with a signal-to-noise ratio greater than 10. They correspond to just over two times the noise in the individual images, and the flux density of the median stack is approximately 12% higher than that of the mean stack. While these are within the error bounds, it implies that the underlying distribution is slightly skewed: there must be more stronger than weaker radio sources.

We therefore performed additional stacks, binning the data into two X-ray luminosity groups (which are essentially also redshift groups). As is shown in Table 1, the radio flux density changes only mildly with X-ray luminosity and corresponds to radio powers around 10^{21}–10^{22} W Hz^{-1}. This is in the star-formation dominated luminosity regime (e.g. Smolčić et al. 2017). To test whether the radio emission in the stacks indeed originates from star-formation, we used the *Spitzer* MIPS 24 μm flux to compute q_{24} parameter values in the FIR-radio diagnostic (e.g. Appleton et al. 2004; Ibar et al. 2008). Nearly all sources (84%) have 24 μm counterparts with flux densities between 20 and 80 μJy, with around 10% of sources in the range 100–300 μJy. These excess sources affect the mean flux density of this distribution, so we instead use the median 24 μm values. In order to establish the latter for each X-ray luminosity bin, we must take the non-detections into account. We employed left-censored survival analysis using a Kaplan-Meier estimator to estimate the

[1] Defined primarily via their wide-band X-ray luminosity (at known redshift): $L_X > 3\times10^{42}$ erg s^{-1}, or $> 3\times10^{35}$ W. This is not a robust lower limit, since (rare) luminous distant starburst galaxies are known to produce $\sim 10^{43}$ erg s^{-1} (Barger et al. 2017). This surface density should be compared to that of faint galaxies, which is $\sim$ 1700 per square arcmin, as inferred for the Hubble Ultra Deep Field (Beckwith et al. 2006).

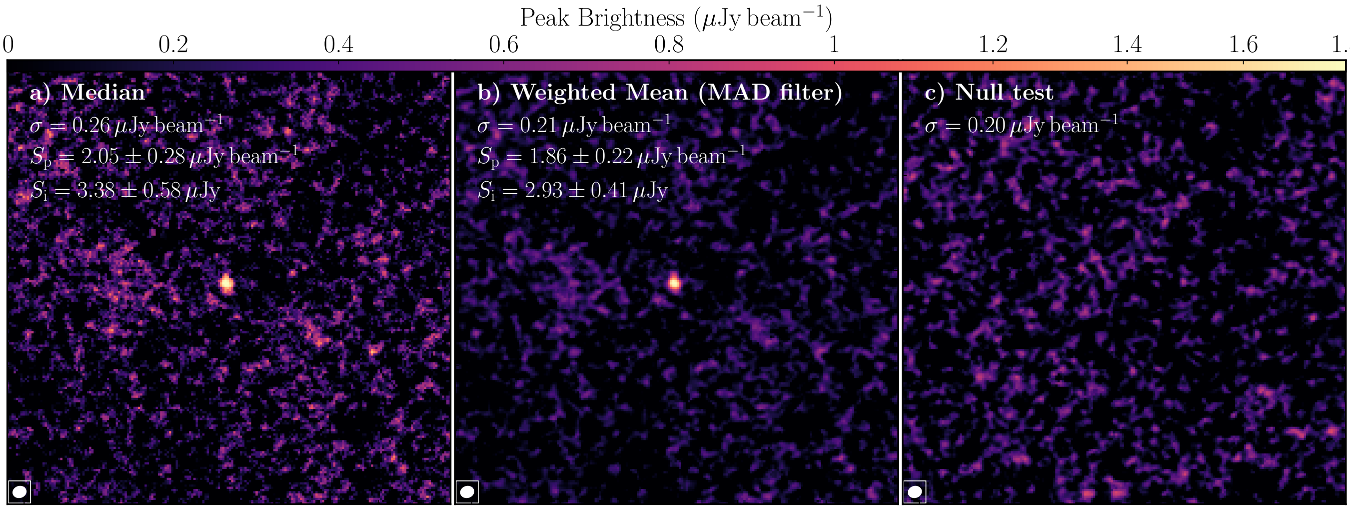

Fig. 1. Stacking results, for 88 objects with X-ray luminosities between 1.9×10^{39} and 4.1×10^{44} erg s^{-1}. The images measure $28'' \times 28''$, with an angular resolution of $\sim 2''$.

median and 95% confidence intervals of the distribution. The results, including the inferred values of radio luminosity and star-formation rate (SFR), are shown in Table 1.

As judged from Table 1 the q_{24} parameter is in the middle of the star-formation dominated regime ($0.2 < q_{24} < 1.5$), both at low and high X-ray luminosities; within the errors they are the same. We tested the sensitivity to redshift of the median q_{24} values for stacks in different redshift intervals and found no effect. We observe no sign of any AGN-driven radio-excess. Recalling the cosmologically remarkable stable q_{24} parameter as measured for star-forming galaxies over a wide range of redshift by Appleton et al. (2004), we therefore suggest that star-formation, with inferred rates of a few to some tens of $M_\odot$ per year, is responsible for (the bulk of) the radio emission of the (sub)μJy population of X-ray selected AGN. These objects are "non-jetted" AGN, in normal star-forming galaxies. We caution nevertheless that we cannot exclude a small level of AGN emission in both the radio and the mid-IR bands: the SFR estimates in the last column of Table 1 must be considered upper limits.

Hereafter defining the "non-jetted" AGN class as having $L_{\rm jet}$ at most 10% of $L_{\rm stack}$ ($L_{1.5\,\rm GHz}$) which translates into $< 3 \times 10^{20}$ W Hz^{-1} at $z = 0.8$ or $< 7 \times 10^{21}$ W Hz^{-1} at $z = 2.2$, we infer that any AGN- or better, jet-driven radio emission, must amount less than about a few times 10^{21} W Hz^{-1}. This represents a factor of about seven orders of magnitude in comparison with the most luminous radio-loud AGN. Given that the q_{24} values are seen not to change with X-ray luminosity (redshift) whereas the radio luminosities do, we measure higher star-formation rates at higher redshift in these AGN hosts – a well-known fact for non-active galaxies (e.g. Whitaker et al. 2012), and for distant radio-loud 3CR objects (Podigachoski et al. 2015).

Figure 2 shows the distribution of the q_{24} values for the 78 individually detected radio sources in the 3–5 sigma set and the 166 objects in the $>$ 5 sigma set together with the two stack values for the radio-undetected X-ray AGN. The grey band indicates the star-formation dominated regime; the area under it is commonly known as the radio-excess region. As seen from Table 1, the mean q_{24} value for the stacked objects is 0.99. The distributions of the q_{24} values for the $>$ 5 sigma and the 3–5 sigma sets are statistically indistinguishable, but the q_{24} values are significantly lower: the combined mean value is 0.73. It is clear that

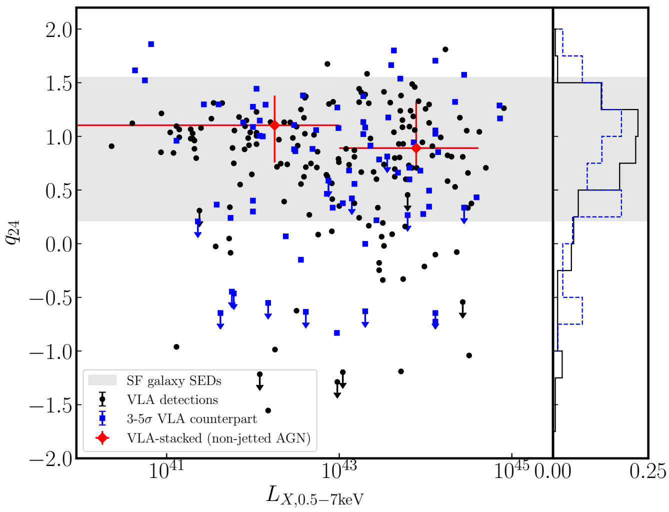

Fig. 2. The FIR/radio ratio, q_{24}, as function of the X-ray luminosity for three groups of X-ray AGN: $>$ 5 sigma VLA detections (black), 3–5 sigma VLA detections (blue), radio-undetected (red); the normalized frequency distributions appear at the right. The grey bar represents the range of q_{24} between redshifts of $0 \le z \le 3$ for five star-forming galaxy templates (data acquired from Del Moro et al. 2013).

the range of 10 μJy–1 μJy marks the transition of jet-dominated to star-formation-dominated X-ray sources: the point has been reached where (any) radio emission is completely dominated by star-formation-related radio processes. Also the radio emission of substantial fractions of the $>$ 5 sigma and 3–5 sigma sets must be largely star-formation-driven. It is noteworthy that this μJy-transition does not come as a surprise since the associated SFRs are entirely as expected (Whitaker et al. 2012). This result recalls earlier work by Richards et al. (2007): from considerably shallower radio data they conclude that a large fraction of X-ray AGN appear as starburst when using radio diagnostics. The $L_{\rm jet}$ upper limits mentioned above are in the range of the faint unresolved radio cores observed (Ho 2008) in low-luminosity AGN[2] in the local universe. We conclude that at least one quarter

[2] But still orders of magnitude more luminous than the ultra-compact radio nucleus in the Galactic Center, Sgr A* (Genzel et al. 2010)

Table 1. Stacking results for two L_X groups of the 88 radio-undetected objects. The 1.5 GHz stack flux densities represent peak values, and the radio luminosity computation assumed a radio spectral index of −0.7. The SFR computation, following Novak et al. (2017), used these luminosity values. The resulting SFR values represent upper limits (see the main text).

$L_{0.5-7\,\mathrm{keV}}$ (erg s^{-1})	N_s	z_{median}	$S_{1.5\,\mathrm{GHz}}$ (μJy beam^{-1})	q_{24}	$L_{1.5\,\mathrm{GHz}}$ (W Hz^{-1})	SFR ($M_\odot$ yr^{-1})
$1.9\times10^{39} - 1.0\times10^{43}$	43	0.75	1.4 ± 0.36	$1.10^{+0.27}_{-0.34}$	3.2×10^{21}	$\lesssim 1.2$
$1.0\times10^{43} - 4.1\times10^{44}$	45	2.18	2.5 ± 0.45	$0.89^{+0.43}_{-0.20}$	6.6×10^{22}	$\lesssim 15$

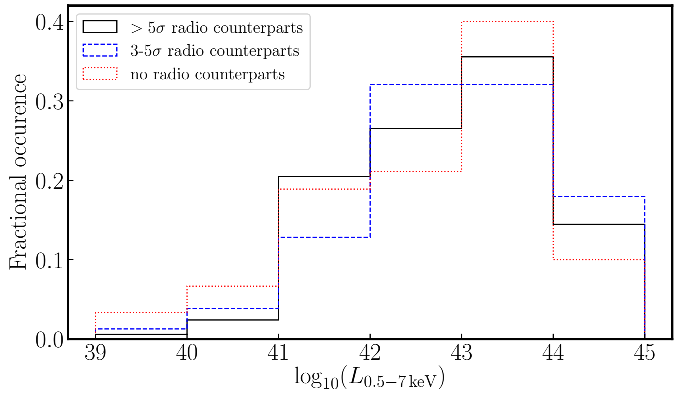

Fig. 3. Histograms of L_X relative frequency, for 3 radio-groups: jet-dominated (black), mixed systems (blue), non-jetted (red).

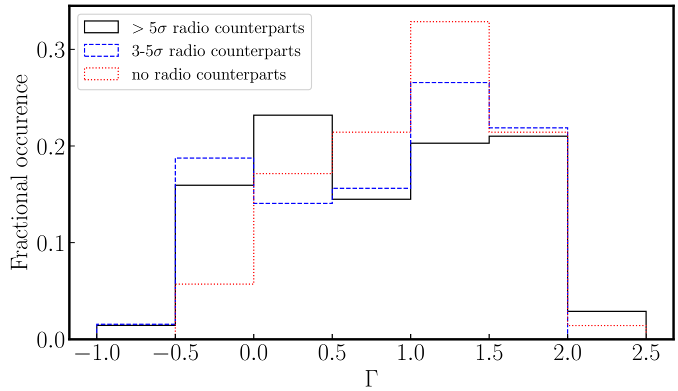

Fig. 4. Histograms of Γ relative frequency for three radio groups: jet-dominated (black), mixed systems (blue), non-jetted (red).

(the stacked set) but probably more like half of the extra-galactic X-ray population has no, or totally insignificant relativistic radio jets with associated AGN-driven radio emission. Following an earlier proposal (Padovani 2017), we classify the radio-silent AGN as "non-jetted" AGN. These objects have an accretion disk and hot corona, hence luminous X-ray emission, but simply do not form radio-jets of any significance.

3. Discussion: the AGN radio source mechanism

We proceed by examining the occurrence of non-jetted AGN in relation to their AGN strength. In Figure 3 we present histograms of the luminosities of three groups of X-ray selected objects: (a) 166 objects in excess of 10 μJy, i.e., the jet-dominated, but still hybrid starburst-AGN group; (b) 78 objects having radio emission in the 5–10 μJy range, i.e., the hybrid starburst-AGN group; (c) the 88 objects without VLA radio emission, i.e., the (stack) radio-silent group.

Kolmogorov-Smirnov tests indicate that these distributions – covering six orders of magnitude in X-ray luminosity – are drawn from the same population, at 99% confidence. This also reflects the fact that the redshift distributions of the three samples are virtually identical. We therefore conclude that X-ray AGN may, or may not, develop jets producing significant radio emission, whose strength is unrelated to the X-ray strength[3]. AGN-driven radio emission – jets, from the pc to the hundreds of kpc scale plus the large-scale radio lobes which they feed – must be simply a special mechanism, unrelated to the strength of the central supermassive black hole accretion as manifested in its emission at other wavelengths. We stress however that some degree of correlation between AGN jet strength and X-ray strength is likely, as a function of black hole accretion efficiency. This is for instance illustrated by the fact that the X-ray luminosities of the ultra-powerful, efficiently accreting 3C sources reach 10^{46}erg s^{-1} (Wilkes et al. 2013), while their histogram shape is similar to those in Figure 3. We furthermore conclude that the level of host starburst contamination at low X-ray luminosities must be similar for the three groups (and we recall the fact that star-forming galaxies have been reported by Barger et al. (2017) to display correlated radio and X-ray luminosities, up to $L_X \approx 10^{42}$ erg s^{-1}. X-ray emitting AGN appear to care little about the presence, or the strength of jet driven radio emission: the two mechanisms are unrelated. Most interestingly, the distributions of the X-ray spectral slopes for the three groups are not exactly the same. Figure 4 shows the effective X-ray photon indices. The radio-silent group peaks at $\Gamma = 1.4$ and shows only a modest tail towards harder photon indices. This is in contrast to the radio-quiet and particularly the radio-loud group, as confirmed with K-S tests. These show pronounced tails of hard photon indices. Such hard indices are generally attributed to the effect of radio jets (Wilkes & Elvis 1987; Zhu et al. 2020), or could indicate different host ISM (absorption) properties (Brandt & Alexander 2015) – clearly an issue for further study.

Our findings are obviously relevant for the local AGN picture, where low luminosity AGN often do not have relativistic radio jets (Ho 2008; Padovani 2017), and as said they provide strong support for the jetted vs. non-jetted scenario (Bonzini et al. 2015; Padovani 2017). Our results presented here have interesting implications. Firstly, the positive stacking signal suggests that many X-ray AGN will have radio counterparts in the nJy sensitivity surveys to be provided by the SKA and ngVLA. Secondly, deeper, more sensitive VLBI observations would be needed to discover radio jets in those objects at the level below 10^{21} W Hz^{-1}. Future surveys will require both deep X-rays and radio observations (sub-arcsecond as well as milliarcsecond resolution) in order to separate the jetted from the non-jetted AGN and to characterise the hybrid AGN-starburst systems. Following up on Garofalo (2019) and Zhu et al. (2020), a multi-spectral ap-

[3] We leave the rare radio-loud blazar class, in which Doppler-boosted jet emission is responsible for strong, variable, correlated emission at all wavelengths outside the present discussion.

proach will be crucial to understand the conditions under which jets will, or will not develop. Finally, ultra-deep optical and infrared observations will be needed to investigate the possible occurrence of non-jetted Compton-thick AGN.

4. Conclusions

At the microJy level, radio surveys run into many star-forming galaxies with SFRs of a few to a few tens of solar masses per year; AGN driven jets contribute negligible amounts of radio emission in these objects. In cases where these jet contributions are non-negligible, a radio excess is apparent, classifying these objects as radio-loud AGN. However, also X-ray AGN without radio jets exist, over a wide range of X-ray luminosity. They represent at least one quarter and probably half of the extra-galactic X-ray population. We have identified their nature: they are core/jet-less (or non-jetted) accretors in massive star-forming galaxies, in which all or virtually all radio emission draws from star-formation related processes in the AGN host galaxy. Whereas their host galaxies generate radio emission, their AGN contribute negligibly – they are radio-silent.

Acknowledgements. The GOODS-N radio sky was addressed in the 2019 PhD Thesis work of author Radcliffe, carried out with the team of co-authors. He and co-author Barthel subsequently examined the radio-invisible population in that field. Barthel wrote the first version of the Article, to which Radcliffe added discussion and diagrams, and to which the other co-authors contributed in its final stage. Barthel and Radcliffe acknowledge useful discussions with Karina Caputi, Luis Ho, Joanna Kuraszkiewicz, Paolo Padovani, and Belinda Wilkes. A useful referee report is also acknowledged.
This research made use of Astropy, a community-developed core Python package for Astronomy (Astropy Collaboration et al. 2013, 2018). It has received funding from the European Commission Seventh Framework Programme (FP/2007-2013) under grant agreement No 283393 (RadioNet3). J.F.R. acknowledges the Science and Technologies Facilities Council (STFC), an Ubbo Emmius scholarship from the University of Groningen, and the South African Radio Astronomy Observatory (SARAO) whose funding contributed to this research.

References

Appleton, P. N., Fadda, D. T., Marleau, F. R., et al. 2004, ApJS, 154, 147
Astropy Collaboration, Price-Whelan, A. M., Sipőcz, B. M., et al. 2018, AJ, 156, 123
Astropy Collaboration, Robitaille, T. P., Tollerud, E. J., et al. 2013, A&A, 558, A33
Barger, A. J., Cowie, L. L., Owen, F. N., et al. 2015, ApJ, 801, 87
Barger, A. J., Cowie, L. L., Owen, F. N., Hsu, L. Y., & Wang, W. H. 2017, ApJ, 835, 95
Barthel, P. D. 2006, A&A, 458, 107
Beckwith, S. V. W., Stiavelli, M., Koekemoer, A. M., et al. 2006, AJ, 132, 1729
Bonzini, M., Mainieri, V., Padovani, P., et al. 2015, MNRAS, 453, 1079
Bonzini, M., Padovani, P., Mainieri, V., et al. 2013, MNRAS, 436, 3759
Brandt, W. N. & Alexander, D. M. 2015, Astronomy and Astrophysics Review, 23, 1
Ceraj, L., Smolčić, V., Delvecchio, I., et al. 2018, A&A, 620, A192
Condon, J. J., Cotton, W. D., Greisen, E. W., et al. 1998, AJ, 115, 1693
Del Moro, A., Alexander, D. M., Bauer, F. E., et al. 2016, MNRAS, 456, 2105
Del Moro, A., Alexander, D. M., Mullaney, J. R., et al. 2013, A&A, 549, A59
Garofalo, D. 2019, ApJ, 876, L20
Genzel, R., Eisenhauer, F., & Gillessen, S. 2010, Reviews of Modern Physics, 82, 3121
Ho, L. C. 2008, ARA&A, 46, 475
Ibar, E., Cirasuolo, M., Ivison, R., et al. 2008, MNRAS, 386, 953
Iglewicz, B. & Hoaglin, D. 1993, How to Detect and Handle Outliers, ASQC basic references in quality control (ASQC Quality Press)
Kellermann, K. I., Condon, J. J., Kimball, A. E., Perley, R. A., & Ivezić, Ž. 2016, ApJ, 831, 168
Lambrides, E. L., Chiaberge, M., Heckman, T., et al. 2020, ApJ, 897, 160
Luo, B., Brandt, W. N., Xue, Y. Q., et al. 2017, The Astrophysical Journal Supplement Series, 228, 2
Mateos, S., Carrera, F. J., Barcons, X., et al. 2017, ApJ, 841, L18
Mauch, T., Cotton, W. D., Condon, J. J., et al. 2020, ApJ, 888, 61
Muxlow, T. W. B., Richards, A. M. S., Garrington, S. T., et al. 2005, MNRAS, 358, 1159
Muxlow, T. W. B., Thomson, A. P., Radcliffe, J. F., et al. 2020, MNRAS, 495, 1188
Novak, M., Smolčić, V., Delhaize, J., et al. 2017, A&A, 602, A5
Owen, F. N. 2018, ApJS, 235, 34
Padovani, P. 2016, A&A Rev., 24, 13
Padovani, P. 2017, Nature Astronomy, 1, 0194
Padovani, P., Mainieri, V., Tozzi, P., et al. 2009, ApJ, 694, 235
Panessa, F., Baldi, R. D., Laor, A., et al. 2019, Nature Astronomy, 3, 387
Podigachoski, P., Barthel, P., Haas, M., Leipski, C., & Wilkes, B. 2015, ApJ, 806, L11
Radcliffe, J. F., Garrett, M. A., Muxlow, T. W. B., et al. 2018, A&A, 619, A48
Richards, A. M. S., Muxlow, T. W. B., Beswick, R., et al. 2007, A&A, 472, 805
Sandage, A. 1965, ApJ, 141, 1560
Smolčić, V., Delvecchio, I., Zamorani, G., et al. 2017, A&A, 602, A2
Whitaker, K. E., van Dokkum, P. G., Brammer, G., & Franx, M. 2012, ApJ, 754, L29
Wilkes, B. J. & Elvis, M. 1987, ApJ, 323, 243
Wilkes, B. J., Kuraszkiewicz, J., Haas, M., et al. 2013, ApJ, 773, 15
Wilson, A. S. 1988, A&A, 206, 41
Xue, Y. Q., Luo, B., Brandt, W. N., et al. 2016, ApJS, 224, 15
Zhu, S. F., Brandt, W. N., Luo, B., et al. 2020, MNRAS, 496, 245